

Logarithmic contribution to the electrical resistivity in $(\text{Ru}_{1-x}\text{Ir}_x)\text{Sr}_2\text{GdCu}_2\text{O}_8$ compoundsS. Garcia,^{1,2} S. Andrade,¹ R. F. Jardim,¹ F. C. Fonseca,³ M. S. Torikachvili,⁴ and A. H. Lacerda⁵¹*Instituto de Física, Universidade de São Paulo, CP 66318, 05315-970 São Paulo, SP, Brazil*²*Instituto de Física, Universidade Federal do Rio de Janeiro, CP 68528, 21941-972 Rio de Janeiro, RJ, Brazil*³*Instituto de Pesquisas Energéticas e Nucleares, 05508-000 São Paulo, SP, Brazil*⁴*Department of Physics, San Diego State University, San Diego, California 92182-1233, USA*⁵*Los Alamos National Laboratory, Los Alamos, New Mexico 87545, USA*

(Received 24 October 2008; revised manuscript received 3 July 2009; published 26 October 2009)

A systematic study of magnetoresistance and dc magnetization was conducted in polycrystalline $(\text{Ru}_{1-x}\text{Ir}_x)\text{Sr}_2\text{GdCu}_2\text{O}_8$ [(Ru,Ir)-1212] compounds, for $0 \leq x \leq 0.15$. We found that a deviation from linearity in the normal-state electrical resistivity (ρ) curves for temperatures below the magnetic transition temperature $T_M < 130$ K can be properly described by a logarithmic term. The prefactor $C(x, H)$ of this anomalous $\ln T$ contribution to $\rho(T)$ increases linearly with the Ir concentration, and diminishes rapidly with increasing applied magnetic field up to $H \approx 4$ T, merging with the $C(0, H)$ curve at higher magnetic fields. Correlation with magnetic susceptibility measurements supports a scenario of local perturbations in the orientation of Ru moments induced in the neighborhood of the Ir ions, therefore acting as scattering centers. The linear dependence of the prefactor $C(x, H=0)$ and the superconducting transition temperature T_{SC} on x points to a common source for the resistivity anomaly and the reduction in T_{SC} , suggesting that the CuO_2 and RuO_2 layers are not decoupled.

DOI: [10.1103/PhysRevB.80.134520](https://doi.org/10.1103/PhysRevB.80.134520)

PACS number(s): 74.72.Jt, 74.25.Fy, 74.25.Ha

I. INTRODUCTION

The intriguing coexistence of superconductivity and magnetic order has placed the ruthenium cuprates under considerable investigation recently.¹ Although a comprehensive understanding of the magnetic response and its correlation with the electric transport properties has been achieved,²⁻⁵ the interplay between the charge carriers and the ruthenium magnetic moments still remains a topic of interest and controversy. Evidence for the scattering of carriers by spin fluctuations was identified from magnetoresistance (MR) data in $\text{RuSr}_2\text{GdCu}_2\text{O}_8$ (Ru-1212).⁶ For temperatures well above the magnetic transition at $T_M \sim 130$ K, the observed negative MR is proportional to the square of the magnetization, and an exchange interaction energy between the conduction electrons and the spin system of ~ 30 meV has been determined.⁶ As T_M is approached from above, the $\text{MR}(T)$ curves become progressively more linear.⁷ Below T_M , a positive peak in $\text{MR}(T)$ emerges at $H \sim 2-3$ T, before becoming negative again in higher magnetic fields.^{6,8} This type of the temperature dependence of MR differs considerably from other Ru oxides, such as SrRuO_3 and $\text{Sr}_4\text{Ru}_3\text{O}_{10}$.⁸

The positive peak in $\text{MR}(T)$ is still not consistently explained. Although qualitative considerations linking the positive peak in MR to either the competition of ferromagnetic and antiferromagnetic interactions,³ or to magnetic phase separation⁹ have been posited, a more detailed understanding is in order. On the other hand, Hall effect and thermopower measurements show an anomalous decrease below T_M .⁴ All these results clearly show that the charge carriers interact with the magnetic moments along the Ru sublattice in the ruthenate cuprates.

In addition to these features, there is an open debate on how conducting the RuO_2 layers are, and to which extent the charge carriers in the layers are delocalized.^{3,4,8} Modeling of

transport properties, based mainly on the Hall effect and thermopower measurements,⁴ suggests appreciable electrical conductivity within magnetically ordered RuO_2 layers, a result supported by band-structure calculations.¹⁰

However, magnetization data¹¹ and nuclear quadrupole resonance¹² results indicate that most of the electronic charge in the RuO_2 layers is localized. A two-band model of parallel conduction in decoupled CuO_2 and RuO_2 layers has been proposed to account for the observed transport properties.^{4,8} Such approach is consistent with the coexistence of magnetism and superconductivity with an exchange interaction of the same order of the superconducting energy gap.⁶ The negative MR and the very large Hall effect strongly point to a small, but appreciable, carrier conduction within the RuO_2 planes, although the main electrical conductivity channel is along the CuO_2 layers.³ These contradictory results and statements clearly indicate that further experimental evidence and a critical analysis of the magnetoresistance data are needed.

In this work we address the coupling between charge carriers and the Ru magnetic moments in the normal state of the $(\text{Ru}_{1-x}\text{Ir}_x)\text{Sr}_2\text{GdCu}_2\text{O}_8$ [(Ru,Ir)-1212] series, in the temperature range between T_M and the superconducting critical temperature T_{SC} . The magnetic and transport properties of the (Ru,Ir)-1212 system were determined as Ir was gradually substituted for Ru up to $x=0.15$. Examining the changes as a function of Ir substitution should lead to a better understanding of the parent material. Iridium has been selected as the doping element in order to locally perturb the Ru magnetic sublattice with negligible structural distortions. $\text{MR}(T)$ measurements, under applied magnetic fields up to $H=18$ T, revealed a logarithmic contribution to the electrical resistivity over a temperature interval of about 30–40 K between T_M and the onset of superconductivity. The magnitude of this anomaly was characterized by a prefactor $C(x, H)$, extracted from fittings of the $\rho(T)$ data.

II. EXPERIMENTAL

Polycrystalline samples of $\text{Ru}_{1-x}\text{Ir}_x\text{Sr}_2\text{GdCu}_2\text{O}_8$ ($0 \leq x \leq 0.15$) were prepared by solid-state reaction, as described elsewhere.¹³ X-ray powder diffraction measurements were performed using $\text{Cu } K\alpha$ radiation on a Brücker D8 Advance diffractometer. The diffraction patterns were collected in the $20^\circ \leq 2\theta \leq 80^\circ$ range with a step size of 0.01° and 8 s counting time. Rietveld refinements of the crystal structures were performed using the GSAS software.¹⁴ The temperature dependence of the magnetoresistance $\rho(x, T, H)$ was measured by the standard four-probe method using a Linear Research Model LR-700 ac bridge operating at 16 Hz. Copper leads were attached to silver-film contact pads on parallelepiped-shaped samples with typical dimensions of $5 \times 2 \times 1.5 \text{ mm}^3$. Magnetoresistance experiments were performed at the National High Magnetic Field Laboratory, Los Alamos, in the temperature range from 2 to 300 K, and magnetic fields H up to 18 T. Measurements of dc magnetization in the remnant field of the superconducting magnet ($H \sim 1 \text{ Oe}$), between 5 and 300 K, upon cooling [field cooled (FC)] and warming [zero-field cooled (ZFC)], were carried out using a superconducting quantum interference device magnetometer from Quantum Design.

III. RESULTS

The x-ray diffraction (XRD) patterns of the (Ru, Ir)-1212 series revealed that all samples were nearly single phase, with small volume fractions ($\leq 2\%$) of SrRuO_3 and $\text{Sr}_2\text{GdRuO}_6$.¹³ The volume fraction of the extra phases is independent of the Ir concentration, within the resolution of the XR diffractometer. The diffraction peaks were indexed as belonging to the Ru-1212 tetragonal phase, space group $P4/mmm$. The lattice parameters and the atomic positions yielded by the Rietveld analysis are independent of the Ir content up to $x=0.10$.¹³ Further details on the structural characterization of this series are described elsewhere.¹³

The temperature dependence of the ZFC and FC magnetization for the pure and 10 at. % Ir-doped samples of this (Ru, Ir)-1212 series are displayed in Fig. 1. The magnetic transition temperature T_M associated with the RuO_2 planes has been determined from the inflection point in the FC curve, i.e., from the maximum in dM/dT . T_M drops linearly with x up to $x=0.10$, as shown in the inset of Fig. 1. While the reduction in T_M for the $x=0.10$ specimen is $\sim 18 \text{ K}$, the value of T_{SC} is $\sim 17 \text{ K}$ lower than for the undoped sample. The smooth separation of the FC and ZFC curves on cooling indicates the emergence of magnetic irreversibility for $T_{\text{irr}} > T_M$, as indicated by the arrows in Fig. 1. This feature is shifted to higher temperatures as x increases, from $T_{\text{irr}}(x=0) \sim 140 \text{ K}$ to $T_{\text{irr}}(x=0.10) \sim 175 \text{ K}$.

Further information regarding the effect of Ir doping on the coupling of the Ru moments can be obtained by examining the magnetic fluctuations above T_M , as seen in the divergence of the magnetic susceptibility. Figure 2 displays a log-log plot of $d\chi/dT$ versus $(T/T_M - 1)$ for the ZFC susceptibility at $T > T_M$. For Ru-1212, a linear behavior has been reported in the $170 \text{ K} < T < 260 \text{ K}$ interval.¹⁵ The value of the slope determined after fitting (~ 2.25) yields a critical

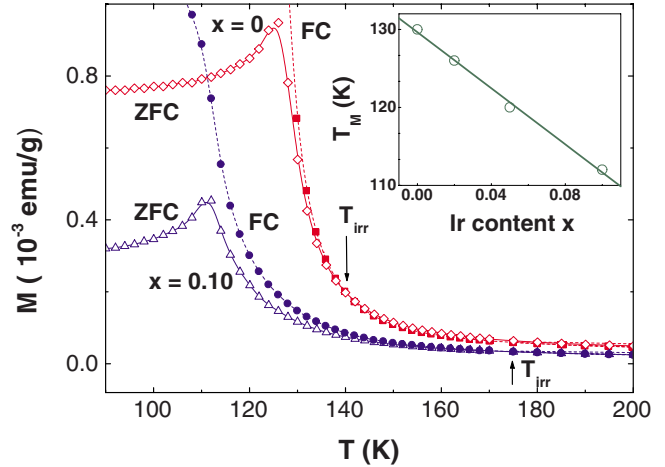


FIG. 1. (Color online) Zero-field-cooled (ZFC, open symbols) and field-cooled (FC, full symbols) magnetization curves for $\text{Ru}_{1-x}\text{Ir}_x\text{Sr}_2\text{GdCu}_2\text{O}_8$ with $x=0$ and 0.10 , measured under the remnant field of the magnet ($H \sim 1 \text{ Oe}$). The beginning of the irreversibility at T_{irr} is indicated by arrows. Inset: the compositional dependence of the magnetic transition temperature T_M .

exponent $\gamma=1.30$ (3), consistent with three-dimensional (3D) XY fluctuations.¹⁵ We obtained the same result for the Ru-1212 sample, by fitting $\chi(T)$ to a straight line in the same temperature range. In addition, the data in Fig. 2 shows that the Ir-doped samples exhibit the same behavior of the parent compound up to $x=0.10$. For $x=0.15$ and 0.20 the linear region gets clearly shorter, showing that the disruption of the Ru sublattice is more significant.

The temperature dependence of the electrical resistivity $\rho(x, T)$ for the studied samples with $H=0$, normalized to their values at 250 K, is presented in Fig. 3. All the curves are linear above $T \sim 180 \text{ K}$. For Ru-1212, the linear depen-

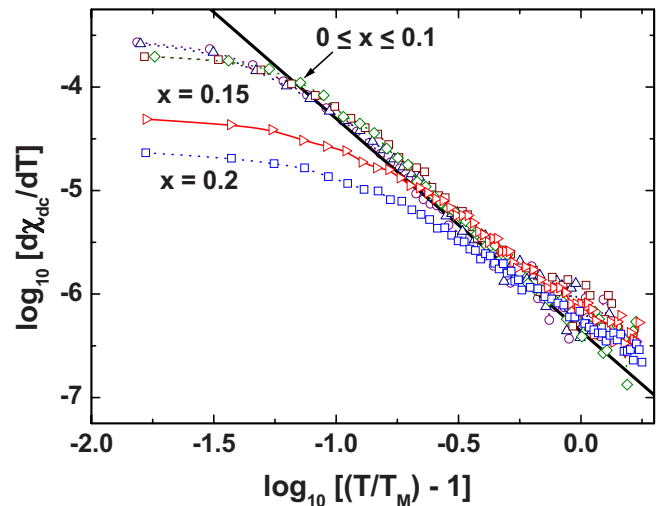


FIG. 2. (Color online) Log-log plot of the derivative of the zero-field-cooled susceptibility $d\chi_{\text{dc}}/dT$ versus $[(T/T_M) - 1]$ above the magnetic transition temperature, T_M , for $\text{Ru}_{1-x}\text{Ir}_x\text{Sr}_2\text{GdCu}_2\text{O}_8$ with $x=0, 0.02, 0.05, 0.10, 0.15$, and 0.20 . The continuous straight line is a fit to the $x=0$ data in the $170 \text{ K} \leq T \leq 260 \text{ K}$ interval. The dotted lines are a guide to the eyes.

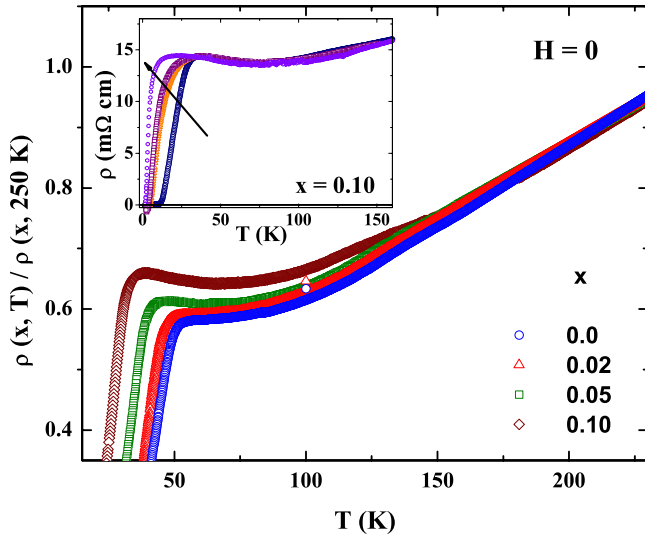


FIG. 3. (Color online) Temperature dependence of the electrical resistivity for $\text{Ru}_{1-x}\text{Ir}_x\text{Sr}_2\text{GdCu}_2\text{O}_8$ with $H=0$ normalized to the values at 250 K. Inset: the electrical resistivity curves for $x=0.10$ and $H=0, 2, 4,$ and 18 T. The arrow indicates increasing magnetic field.

dence is extended down to the neighborhood of T_M , where a subtle anomaly is observed.⁶ The temperature range in which the linear behavior takes place is gradually shortened as x increases, and it coincides with the T range of the reversible region of the ZFC-FC magnetization curves (Fig. 1). Upon cooling below T_{irr} , a smooth upward departure from linearity is detected. The deviation from linearity is larger for higher x values. The electrical resistivity increases as the temperature is decreased below T_M , and a minimum is developed for $x=0.05$ and 0.10 . On further cooling, the onset of the superconducting state at T_{SC} is reached. The resistivity curves with $H>0$ exhibit a similar behavior, as shown in the inset of Fig. 3 for $x=0.10$. The deviation from linearity and a shallow minimum again emerge upon cooling. We note that even for the higher Ir content ($x=0.1$) and $H=18$ T, the zero-resistance value is reached without broadening in the superconducting transition.

The reason for the rise in the electrical resistivity can be, in principle, inferred from its temperature dependence. First, it is possible that the upturn in $\rho(T)$ is due to semiconducting behavior or a variable-range hopping process. The electrical resistivity associated with these mechanisms would result in a temperature dependence as $\rho \sim \exp(T^{-\alpha})$, with $\alpha=1, \frac{1}{4}$, and $\frac{1}{2}$ corresponding, respectively, to activation, uncorrelated, and correlated variable-range hopping processes.¹⁶ None of these functional forms fit the divergence in the electrical resistivity in the whole temperature interval. A power-law dependence ($\ln \rho \sim \ln T$) also failed to describe the experimental data. Since a logarithmic contribution to the resistivity has been observed on cooling in different cuprates^{17–19} a

$$\rho(x, H, T) = A + BT - C \ln T \quad (1)$$

dependence was considered. The coefficients A and B were determined by fitting straight lines to the experimental data

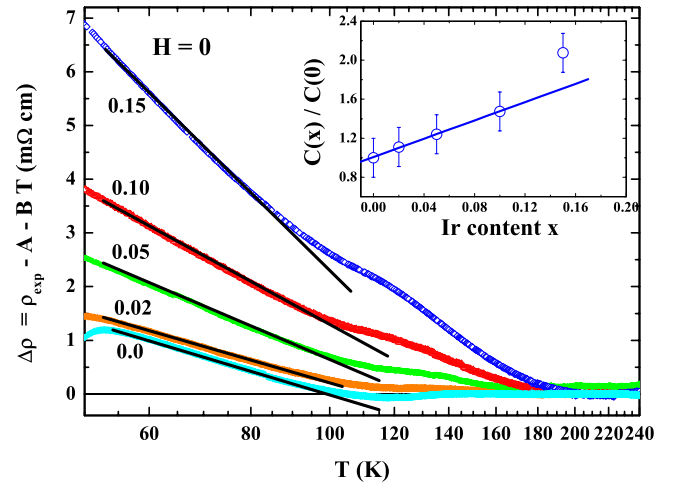


FIG. 4. (Color online) Dependence of the nonlinear part of the electrical resistivity $\Delta\rho = \rho_{\text{exp}} - A - BT$ on $\ln T$ for $\text{Ru}_{1-x}\text{Ir}_x\text{Sr}_2\text{GdCu}_2\text{O}_8$ at $H=0$ T. The coefficients A and B were determined as described in the text. The solid straight lines are fits to the data. The values of the slope rise with increasing x and correspond to the prefactor C in Eq. (1). Inset: the compositional dependence of the prefactor $C(x)$ normalized to the $C(0)$ value for $H=0$. The continuous straight line is a fit for $x \leq 0.10$.

in the linear region. The deviation from linearity, $\Delta\rho = \rho_{\text{exp}} - A - BT$, is plotted against $\ln T$ (on a log scale) in Fig. 4 for $H=0$ T. A linear behavior is observed for $T_{\text{SC}} < T < T_M$, i.e., an interval of about 30–40 K. In addition, the slope of the $\Delta\rho$ versus $\ln T$ curves was found to increase with Ir concentration. The values of the prefactor $C(x, H=0)$ were obtained from the fitting procedure, in the linear portion of the $\Delta\rho$ versus $\ln T$ curves. Their compositional dependence, normalized to the $C(0, 0)$ value, is shown in the inset of Fig. 4. Up to $x=0.10$, the ratio $C(x, 0)/C(0, 0)$ increases linearly with x , and it deviates upwards for higher concentrations $x>0.10$. No specific type of dependence was found for the $T_M \leq T \leq T_{\text{irr}}$ interval.

The $\Delta\rho$ versus $\ln T$ plots under applied magnetic fields $H>0$ were found to exhibit a similar trend, and the magnetic field dependence of the extracted prefactor $C(x, H)$ is displayed in Fig. 5. As the magnetic field is increased, the prefactor $C(x, H)$ decreases monotonically up to $H \approx 3-4$ T. At higher magnetic fields, the $C(x, H)$ vs H curves merge. For the $C(0.10, H)$ curve, a small difference with the $C(0, H)$ values for the highest applied magnetic field ($H=18$ T) still remains.

The inset of Fig. 5 displays the magnetic field dependence of the relative change in the electrical resistivity $\Delta\rho(H)/\rho(H=0 \text{ T})$, with $\Delta\rho(H) = [\rho(H) - \rho(H=0)]$, at $T=70$ K, for samples with $x=0$ and 0.10 . A smooth maximum is observed in the $H \sim 3-4$ T range for both curves, i.e., the same magnetic field region in which changes in the decreasing rate of the $C(x, H)$ coefficients were observed. The broad peak in $\Delta\rho(H)/\rho(H=0 \text{ T})$ shifts slightly to higher fields and shows an increase in its amplitude for the specimen with $x=0.10$.

In order to investigate further the interplay between magnetic interactions and the conduction mechanism, we at-

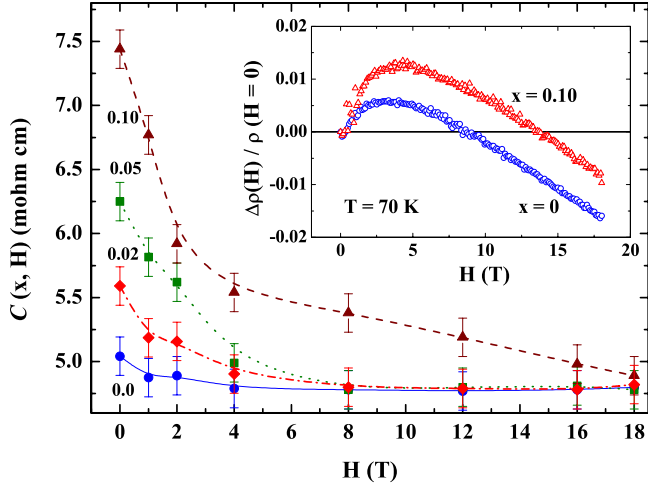


FIG. 5. (Color online) Magnetic field dependence of the prefactor $C(x, H)$ in Eq. (1) for $\text{Ru}_{1-x}\text{Ir}_x\text{Sr}_2\text{GdCu}_2\text{O}_8$ with $x=0$ and 0.10 . The lines are a guide to the eyes. Inset: the field dependence of the relative change in the electrical resistivity $\Delta\rho(H)/\rho(0)$ at $T=70$ K.

tempted to correlate the prefactor $C(x, H)$ with the magnetic susceptibility. The FC magnetization curve for the parent Ru-1212 compound, $M(0, T)$, was subtracted from the $M(x, T)$ values for the Ir-substituted compounds. The resulting $\Delta M(x, T) = M(x, T) - M(0, T)$ curves for $T > T_M$ are shown in Fig. 6. These curves resemble a Curie-type dependence, possibly associated with some local induced magnetic moment promoted by the Ir substitution. Assuming the emergence of such local moments, we have plotted $1/\chi_{\text{dc}}$ versus T , as shown in the inset of Fig. 6, to determine the corresponding Curie constants $D_{\text{ind}} = N\mu_{\text{ind}}^2/3k_B$. Here, N is the density of Ir ions per unit volume, μ_{ind} is the induced local magnetic moment, and k_B is the Boltzmann constant. The validity of this approach is of course limited to the extent to which the temperature-independent contributions to the susceptibility

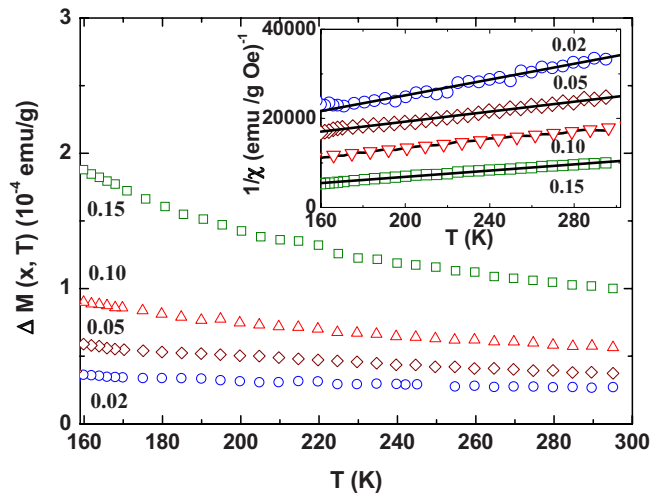


FIG. 6. (Color online) Temperature dependence of the difference $\Delta M(x, T)$ between the field-cooled magnetization curves for the Ir-substituted samples and the parent compound in $\text{Ru}_{1-x}\text{Ir}_x\text{Sr}_2\text{GdCu}_2\text{O}_8$. Inset: $1/\chi_{\text{dc}}$ versus T plots using the $\Delta M(x, T)$ data. The straight lines are linear fits for $T \geq T_{\text{irr}}$.

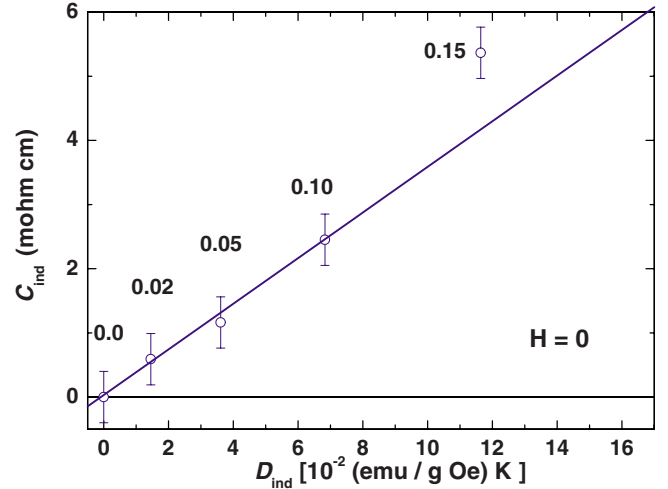


FIG. 7. (Color online) Dependence of the prefactor C_{ind} on the Curie constant D_{ind} . The values of D_{ind} were obtained from fits to χ^{-1} vs T (inset of Fig. 6). C_{ind} represents the net contribution to the logarithmic divergence in the electrical resistivity associated with the Ir doping (see text for details).

$\chi_0(x)$ (core diamagnetism, Van Vleck, and Pauli paramagnetic terms) are canceled by subtraction. The typical values for these contributions in the high- T_C cuprates^{20,21} are two orders of magnitude lower than the Curie contribution at the highest temperature considered (300 K) for the sample with the smaller D_{ind} value ($x=0.02$). Therefore, any possible contribution to $\Delta M(x, T)$ due to differences in $\chi_0(x)$ associated to doping is washed out by the Curie component. D_{ind} was extracted from the slope of the straight lines fitted for temperatures above the corresponding T_{irr} . Since the parent Ru-1212 compound exhibits a nonzero $C(0, 0)$ value, it has been subtracted from the $C(x, 0)$ in order to obtain a new prefactor $C_{\text{ind}} = C(x, 0) - C(0, 0)$ describing the net contribution to the logarithmic deviation from linearity associated with the Ir content. These prefactors were found to vary linearly with D_{ind} , as shown in Fig. 7, except for the sample with $x=0.15$, where a clear deviation from the linear dependence is actually observed. The obtained values of μ_{ind} , deduced from the D_{ind} parameters, ranged from ~ 30 to $\sim 50\mu_B$, for samples with $x=0.02-0.10$, respectively.

IV. DISCUSSION

Deviations from linearity in the $\rho(T)$ curves have been observed for the ruthenate cuprates and ascribed to low-quality intergranular junctions.^{22,23} Several observations indicate that this is not the case for the (Ru, Ir)-1212 materials of this study. First, the volume fraction of the stray secondary phases observed in the XRD patterns is essentially constant for all the samples. Therefore, no differences are induced in the intergranular composition by Ir doping. Secondly, the increase in the deviation with the Ir content is not accompanied by suppression of superconductivity or broadening of the resistive transition, as shown in the inset of Fig. 3, with all the samples reaching zero resistance, even for fields as high as $H=18$ T. Finally, the departure from linearity is ex-

pected to increase with the rise in H as T_{SC} is approached for the case of dominant weak-links effects, since a fraction of the superconducting junctions at $H=0$ or at low fields will evolve to the normal state as H increases.

The emergence of the deviation from linearity in the resistivity curves correlates well in temperature with the appearance of irreversibility in the magnetization measurements, suggesting a magnetic origin for this behavior. The suppression of the divergence as the magnetic field is increased, as well as the correlation between the prefactors C and the Curie-Weiss constants D_{ind} in the Ir-doped materials, strongly support this interpretation.

Other possible sources for the $\ln T$ behavior are weak localization²⁴ and two-dimensional electron-electron interaction.²⁵ However, these two mechanisms are directly related to the effects of structural disorder. Since Ir doping leaves the atomic positions and lattice parameters unchanged up to $x=0.10$, they do not apply to the (Ru,Ir)-1212 series. This is supported by the fact that the values for the prefactor of the $\ln T$ term are much smaller than those expected from both theories, which predict that whenever the conductance is $>e^2/h$ ($R < 25 \Omega$, a condition met by all our samples), the coefficient of the $\ln T$ conductance should be around e^2/h . The values for the coefficients C are about a few $m\Omega$ cm, as shown in Fig. 5. The corresponding values for the conductance are almost one order of magnitude smaller in comparison to the predicted ones. Finally, it has been shown that these two scattering channels are inconsistent with negative magnetoresistance,^{17,18} as observed for the (Ru,Ir)-1212 system.

The values of μ_{ind} obtained from the $\chi(T)$ data, ranging from ~ 30 to $\sim 50\mu_B$ as the concentration of Ir increases, suggest a scenario in which magnetic clusters act as scattering centers in the Ir-substituted samples. We recall here, however, that the prefactor C is not zero for the parent Ru-1212 ($x=0$) compound and that the logarithmic contribution to the electrical resistivity is detected for the same temperature interval as that observed for the doped samples (Fig. 4). It is interesting to note from the inset in Fig. 4 that the linear behavior obtained for the compositional dependence of the normalized prefactors with $H=0$, includes the point $C(x)/C(0)=1$ for $x=0$, a result by no means trivial. Also, its variation with the magnetic field (Fig. 5) is consistent with the sequence of curves obtained for $x>0$. These results strongly suggest the presence of intrinsic magnetic clusters in Ru-1212 ($x=0$) and that Ir doping promotes their formation. The existence of nanomagnetic clusters in Ru-1212 has been proposed to account for superparamagnetic $M(H)$ curves and slow spin dynamics effects.⁷ Nonlinear ac magnetic susceptibility measurements support this assumption.²⁶ These data suggest that the clusters act as intrinsic scattering centers in the parent Ru-1212 compound, and their density and size increase with the rise in x . As H is increased, the scattering of the charge carriers by the magnetic clusters decreases, as they become gradually coupled to the magnetic field. The enhancement of magnetic-cluster formation by Ir doping is possibly related to the similar electronic configuration of Ru($4d^75s^1$) and Ir($5d^75s^2$), favoring some coupling of the Ir magnetic moments to the Ru spin system. This coupling locally perturbs the orientation of the neighboring

Ru moments within a certain correlation volume of nanometric size, leaving essentially unchanged a significant fraction of them in the Ru-1212 matrix. The fact that Ir substitution up to $x=0.10$ does not alter a distinct feature of the magnetic response of Ru-1212, as the 3D XY character of the magnetic fluctuations above T_M (Fig. 2), indicates that the interplane coupling between the RuO₂ layers and the orientation of most of the Ru moments parallel to them, are not affected by the Ir content in the range studied, supporting the idea that the magnetic perturbation associated to doping has a local character. The low decreasing rate of T_M for $x \leq 0.10$ also indicates that the disruption of the Ru sublattice is moderate. For comparison, while $T_M=112$ K for $x(\text{Ir})=0.10$, the value of T_M for the same at. % Sn-substitution is about 30 K lower, suggesting a much stronger disruption of the magnetic correlations within the Ru sublattice.²⁷ We note that Sn is a diamagnetic species that simply dilutes the Ru-spin system, leaving practically unchanged the volume of the unit cell for 10% substitution (the actual change is $\sim 0.15\%$).

A logarithmic contribution to the electrical resistivity has been reported for different high- T_C cuprates,^{16–19,28} and scattering by magnetic centers was identified as the source of the anomaly. Local magnetic moments were induced in the CuO₂ conduction planes by Cu substitution or promoted through localization of holes due to disorder. The situation is quite different for (Ru,Ir)-1212, where the perturbation of the magnetic order is located in the adjacent RuO₂ layers, while the CuO₂ planes are not affected. Therefore, either the RuO₂ planes are conducting below T_M and/or the charge carriers are not confined to the CuO₂ planes. Since no distortions are induced by Ir doping, the decrease in T_{SC} is not due to structural disorder. The fact that the prefactor $C(x,H)$ and T_{SC} exhibit a linear dependence on x strongly suggest that the interaction of carriers with the spin system in the normal state has a leading role in T_{SC} suppression, indicating that the RuO₂ and CuO₂ planes are not decoupled.

V. CONCLUSIONS

A logarithmic deviation from linearity in the normal-state region of the resistivity curves in (Ru,Ir)-1212 is due to the interaction of the charge carriers with the ordered Ru sublattice. The compositional and magnetic field dependence of the coefficients of the logarithmic contribution strongly suggest a scenario of intrinsic magnetic clusters acting as scattering centers in the parent Ru-1212 ($x=0$) compound, with density and size that increase upon Ir substitution. Cluster formation is promoted by a local perturbation in the orientation of the Ru magnetic moments in the neighborhood of the Ir ions. The role of the spin degrees in the conduction mechanism is clearly evidenced by the progressive suppression of this scattering channel with increasing magnetic field and by its strengthening with the increase in the density and size of the scattering centers. The correlation between the intensity of the resistivity anomaly and the decrease in the superconducting transition temperature strongly suggests that the interaction that scatters the charge carriers in the normal state is the dominant pair-breaking mechanism and evidences that a fraction of the carriers entering into the superconducting state interacts with the Ru moments.

ACKNOWLEDGMENTS

This work was supported by the Brazilian Agencies FAPESP under Grants No. 05/53241-9 and No. 07/51458-6, CNPq under Grant No. 473932/2007-5, and by the US National Science Foundation under Grants No. DMR-0306165

and No. DMR-0805335 (M.S.T). S.G. acknowledges financial support from FAPERJ (Grant No. E26/100.092/2009). Work at the NHMFL was performed under the auspices of the NSF, the State of Florida, and the U.S. Department of Energy.

-
- ¹T. Nachtrab, C. Bernhard, L. Chengtian, D. Koelle, and R. Kleiner, *C. R. Phys.* **7**, 68 (2006).
- ²S. García, J. E. Musa, R. S. Freitas, and L. Ghivelder, *Phys. Rev. B* **68**, 144512 (2003).
- ³M. Pozek, I. Kupcic, A. Dulcic, A. Hamzic, D. Paar, M. Basletic, E. Tafra, and G. V. M. Williams, *Phys. Rev. B* **77**, 214514 (2008).
- ⁴J. E. McCrone, J. L. Tallon, J. R. Cooper, A. C. MacLaughlin, J. P. Attfield, and C. Bernhard, *Phys. Rev. B* **68**, 064514 (2003).
- ⁵S. García and L. Ghivelder, *Phys. Rev. B* **70**, 052503 (2004).
- ⁶J. E. McCrone, J. R. Cooper, and J. L. Tallon, *J. Low Temp. Phys.* **117**, 1199 (1999).
- ⁷Y. Y. Xue, F. Chen, J. Cmaidalka, R. L. Meng, and C. W. Chu, *Phys. Rev. B* **67**, 224511 (2003).
- ⁸M. Pozek, A. Dulcic, D. Paar, A. Hamzic, M. Basletic, E. Tafra, G. V. M. Williams, and S. Kramer, *Phys. Rev. B* **65**, 174514 (2002).
- ⁹B. Lorenz, Y. Y. Xue, R. L. Meng, and C. W. Chu, *Phys. Rev. B* **65**, 174503 (2002).
- ¹⁰K. Nakamura, K. T. Park, A. J. Freeman, and J. D. Jorgensen, *Phys. Rev. B* **63**, 024507 (2000).
- ¹¹T. P. Papageorgiou, E. Casini, Y. Skourski, T. Herrmannsdörfer, J. Freudenberger, H. F. Braun, and J. Wosnitza, *Phys. Rev. B* **75**, 104513 (2007).
- ¹²Y. Tokunaga, H. Kotegawa, K. Ishida, Y. Kitaoka, H. Takagiwa, and J. Akimitsu, *Phys. Rev. Lett.* **86**, 5767 (2001).
- ¹³A. Jurelo, S. Andrade, R. F. Jardim, F. C. Fonseca, M. S. Torikachvili, A. H. Lacerda, and L. Ben-Dor, *Physica C* **454**, 30 (2007).
- ¹⁴A. C. Larson and R. B. Von Dreele, Los Alamos National Laboratory Report No. LAUR 86-748, 2000 (unpublished).
- ¹⁵C. Bernhard, J. L. Tallon, Ch. Niedermayer, Th. Blasius, A. Golnik, E. Brücher, R. K. Kremer, D. R. Noakes, C. E. Stronach, and E. J. Ansaldo, *Phys. Rev. B* **59**, 14099 (1999).
- ¹⁶G. Xiao, M. Z. Cieplak, and C. L. Chien, *Phys. Rev. B* **40**, 4538 (1989).
- ¹⁷T. W. Jing, N. P. Ong, T. V. Ramakrishnan, J. M. Tarascon, and K. Remschnig, *Phys. Rev. Lett.* **67**, 761 (1991).
- ¹⁸N. W. Preyer, M. A. Kastner, C. Y. Chen, R. J. Birgeneau, and Y. Hidaka, *Phys. Rev. B* **44**, 407 (1991).
- ¹⁹Y. Ando, G. S. Boebinger, A. Passner, T. Kimura, and K. Kishio, *Phys. Rev. Lett.* **75**, 4662 (1995).
- ²⁰D. C. Johnston, *Phys. Rev. Lett.* **62**, 957 (1989).
- ²¹D. C. Johnston, *J. Magn. Magn. Mater.* **100**, 218 (1991).
- ²²M. Pozek, A. Dulcic, D. Paar, G. V. M. Williams, and S. Kramer, *Phys. Rev. B* **64**, 064508 (2001).
- ²³J. L. Tallon, J. W. Loram, G. V. M. Williams, and C. Bernhard, *Phys. Rev. B* **61**, R6471 (2000).
- ²⁴P. A. Lee and T. V. Ramakrishnan, *Rev. Mod. Phys.* **57**, 287 (1985).
- ²⁵B. L. Altshuler and A. G. Aronov, in *Electron-Electron Interaction in Disordered Systems*, edited by M. Pollak and A. L. Efros (North-Holland, Amsterdam, 1985), pp. 1–53.
- ²⁶M. R. Cimberle, R. Masini, F. Canepa, G. Costa, A. Vecchione, M. Polichetti, and R. Ciancio, *Phys. Rev. B* **73**, 214424 (2006).
- ²⁷A. C. McLaughlin and J. P. Attfield, *Phys. Rev. B* **60**, 14605 (1999).
- ²⁸A. T. Fiory, S. Martin, R. M. Fleming, L. F. Schneemeyer, and J. V. Waszczak, *Phys. Rev. B* **41**, 2627 (1990).